Imaging of flange bore internal defects using phased array ultrasonic testing

L Penaluna, P Charlton, S Mosey and J Jenkins

The ability of phased array ultrasonic testing (PAUT) to adapt to a large range of applications has led to its prevalence within the non-destructive testing (NDT) industry. There are, however, demonstrated weaknesses in its use when inspecting non-parallel surfaces with unknown dimensions. One such example is flange bore inspection. Utilising simulation and real-world testing, this paper proposes and evaluates the use of a wide-angled sweep method, used in conjunction with compound scan imaging for flange bore inspection. It is concluded that the wide-angle sweep method is capable of determining the required parameters to allow for inspection and that compound scan imaging provides the best means of visualisation for defect detection and sizing.

1. Introduction

Phased array ultrasonic testing (PAUT) has become a widespread and versatile inspection solution for many non-destructive testing (NDT) applications. It is, however, not without its limitations. One such limitation becomes apparent when inspecting complex geometries. Due to the nature of sound propagation, at any time at which unknown angles are encountered with non-parallel surfaces, it is possible for a large proportion of the energy to be directed away from the receiving probe[1].

Used for many years in the medical field[2], the compound S-scan is still a relatively new but growing inspection strategy within NDT. Currently, it is used almost exclusively for weld inspection in conjunction with an angled wedge[3].

According to[2] the medical field benefits from utilisation because 'compounding improves the acquisition of echoes from specular targets by changing the orientation of the insonifying beam and also reduces the speckle noise in greyscale images. These gains are achieved while maintaining the high resolution and flexibility of a computer-controlled phased array sector scanner'. It is for these reasons that it is suggested that compound scans will allow for the inspection of non-parallel surfaces. By insonifying defects with sound from multiple angles, the chance of a reflected beam returning to the probe greatly increases.

2. Flange bore inspection

A pipe flange is a disc, collar or ring that attaches to a pipe with the possible purpose of providing increased support for strength, blocking off a pipeline or, most commonly, joining two pipe sections together. Typically, they are welded to the pipe ends and secured together with the use of long bolts. A gasket is often inserted between the two mating flanges to provide a tighter seal. Figure 1 shows a typical example.

To increase strength, there is a region where a flange tapers out from the diameter of the pipe to a larger diameter near the mating face. This means that in this area the internal and external surfaces are non-parallel and at an unknown angle. The distances between the surfaces, which will change across the taper, are also unknown. These angles and depths provide crucial information in the selection of PAUT set-up parameters.

Image resolution is highly dependent on proper focusing and this can be difficult to achieve, even when geometries are known.

While probability of detection is greatly influenced by correct focusing, in[4] it is concluded that: 'It is impossible to derive standard formula that could provide selection of focal law parameters. However, from simulation software, one can achieve effective selection of focal law parameters.' This implies that even when angles are known, simulation is still required to find optimal focal laws.

Correct steering is of even greater importance. As shown in Figure 2, even a fairly wide-angled sectorial sweep that is directed
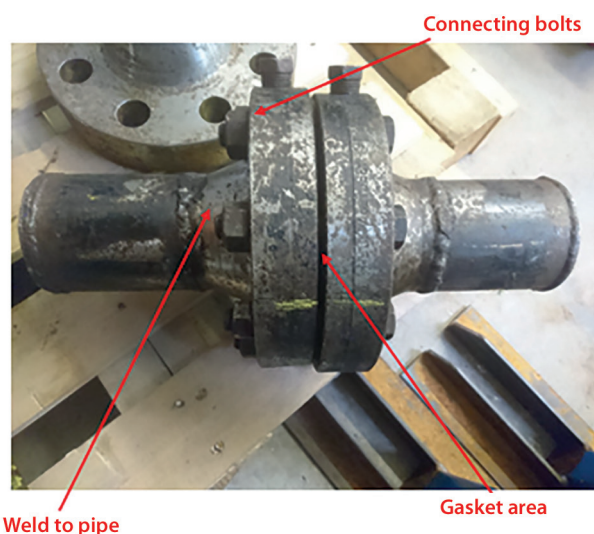

Figure 1. Example of a flange

Connecting bolts

Gasket area

Weld to pipe

incorrectly can return no signal whatsoever from the flange bore, as the sound is reflected towards the flange face and away from the probe.
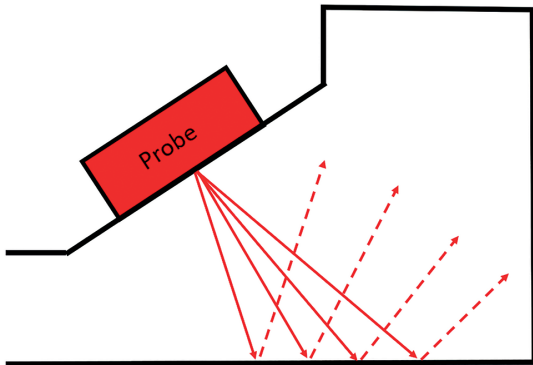

Figure 2. Reflection away from the bore

The current industry-standard NDT technique for the evaluation of a flange uses a shear wave sector scan that is produced at a high angle (often aided by a wedge) and introduced into the component either through the bolting area or the flange skirt[5]. This is displayed in Figure 3.
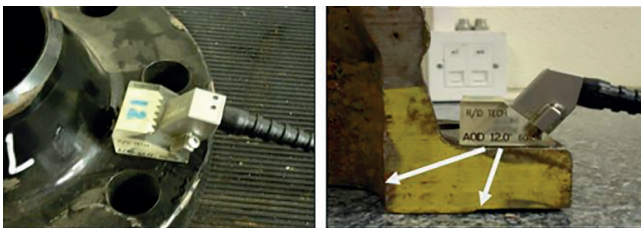

Figure 3. Flange face inspection[5]

As shown in Figure 4, the beam is reflected back to the probe from the raised sealing face, the flange corner and any corrosion between these two points.
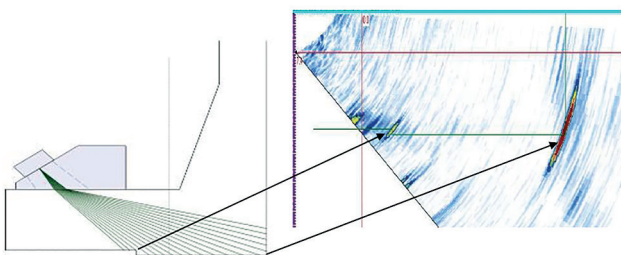

Figure 4. Response from face inspection[5]

A wide range of techniques can also be applied to test for corrosion within the weld that joins the flange to the pipe. It is currently assumed that if the flange face and weld areas are in good order, then so too is the flange bore.

As can be seen in Figure 5, the flange face is in excellent condition and minimal corrosion has occurred around the weld; the bore, however, has extensive corrosion that ultimately led to its failure.

The US Department of Transportation's Pipeline and Hazardous Materials Safety Administration[6] records for 2016 show that in the first six months of that year 12 spillages from pipelines occurred. This resulted in an estimated 166,000 gallons of oil product and an

unknown quantity of toxic gases, such as propane and butane, being released into the environment. Even worse, on 12 April of that year, a leak in a pipe at a gas plant in Woodsboro, Texas, USA, led to an explosion that resulted in the death of two people.

Figure 5. Bore corrosion

The fact that each of these cases occurred in just a single six-month period and within the USA, where regulations, quality control and testing standards are significantly higher than many parts of the world, highlights the importance of NDT. It is not known how many of these cases were directly linked to corrosion within the flange bore, but the seriousness of having untested areas is clear.

The work presented in this paper uses flange bores to provide examples involving complex geometry and shows the development and validation of a method that allows for the entirety of a flange bore to be tested. This method can potentially be modified and applied to other components that are not currently suitable for ultrasonic inspection.

3. Simulation

3.1 Wide sweep method (WSM)

The first challenge to overcome is determining the angle at which the bore is offset in relation to the surface. One way to accomplish this would be to find the manufacturer of each individual flange that would ever require inspection and try and obtain data from them. This would be a laborious, time-consuming process and may not even be possible. It is highly likely that with older pipeline manufacturers some may have since gone out of business and therefore no records would be available for the particular flange design needed.

It would also be possible to slowly build up a database of all flanges requiring inspection by taking them out of service and undertaking physical measurements. In[7], the average cost of a pipeline shutdown is predicted to be in excess of £2 million per day. As the entire goal of utilising NDT is to increase safety while preventing these costly shutdowns wherever possible, this is most definitely not desirable.

As an NDT system is already going to be implemented (in this case PAUT), it makes most sense to try and use that system to determine the angle and depth measurements. The proposed solution is to perform a complete (or close to) 180° sectorial scan with the probe in the position at which it will be scanning.

As illustrated in Figure 6, a single ray of sound travelling through a medium can be said to travel in a straight line. If it were to reflect off a boundary, the angle of reflection would be equal to that of incidence. This means that when multiple beams exit the

probe at varied angles, any that come into contact with a boundary that is not 90° relative to the probe will be reflected away and not return to the probe. Therefore, when a large sectorial sweep of 180° (or close to this) is performed from the flange skirt, only the angle at which the flange bore is at a normal will receive a signal. The angle at which this occurs will allow the face-to-bore angle to be established. Additionally, by recording the time taken for the signal to return, the probe centre-to-bore distance can be determined.
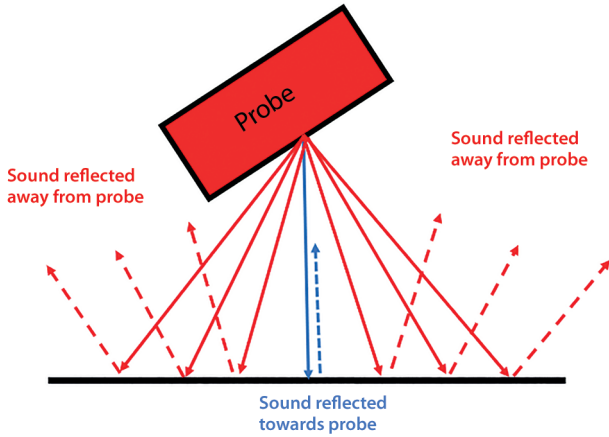

Figure 6. Signal returned at normal

In order to evaluate the ability of the proposed method to accurately determine the depth and angle, a series of simulations were performed using the CIVA ultrasonics software package. A real-world flange geometry was modelled using the SolidWorks CAD program and then imported into CIVA. This flange was selected due to its median size and geometry and is shown along with its CAD model in Figure 7.

Figure 7. Flange model

Although it would be possible to just conduct physical testing, all responses would have to be assumed to be the flange bore. The CIVA results provide a better understanding of the beam and its interactions. This is also a good opportunity to validate CIVA by comparing the output results with those from real-world inspection.

The simulation utilises a Zetec LM 5 MHz probe (characteristics are given in Table 1) performing a longitudinal wave sectorial scan with a 178° sweep (−89° to 89°) and transmitting/receiving on all 64 elements. The flange material is carbon steel with a compression wave velocity of 5960 m/s.

Table 1. Characteristics of a Zetec LM 5 MHz probe

Part ID	Frequency (MHz)	Number of elements	Primary axis pitch (mm)	Primary aperture (mm)	Secondary aperture (mm)
LM 5 MHz	5	64	0.6	38.4	10

3.2 Results

Figure 8 highlights the usefulness of CIVA over real-world testing alone. Unlike the real world, it is possible to have an overlay of the flange that shows where any signal responses are coming from. Key areas have been noted.
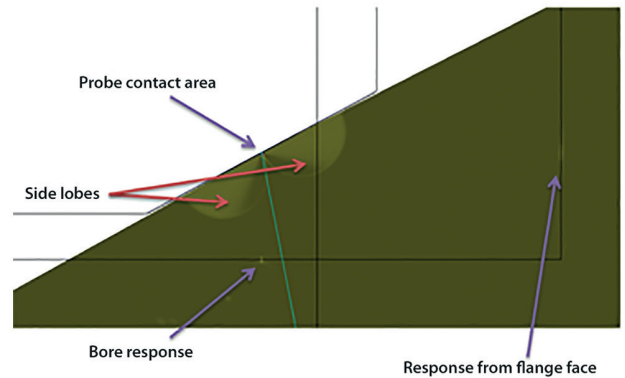

Figure 8. CIVA response

Figure 9 shows an S-scan image that is representative of real-world testing, although the range has been increased to a value far in excess of that which would be required. This is to show the full extent of the signals that could be received and to demonstrate that the flange bore could easily be identified even if an operator were to use such a large range.
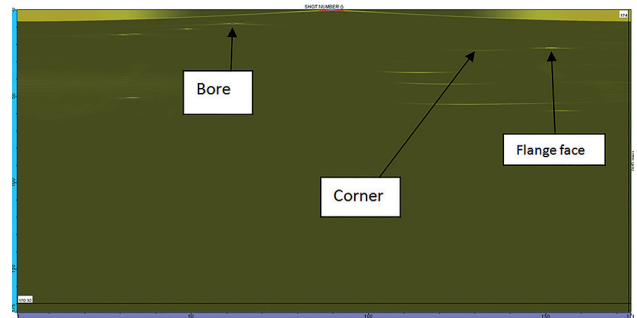

Figure 9. Excess range S-scan

Figure 10 shows that by reducing the time base to a more reasonable value a result can be observed that mimics the response that an operator would be looking for. By comparing this to the output from the WSM performed on the real flange, it can be seen that a high level of correlation is present.

3.3 Discussion

From research into flange design specifications it becomes apparent that for pipe walls of thickness, the flange bolting area must be even thicker[8]. This is beneficial to this method as it predicts that the response from the flange face should always appear at a greater depth to that of the flange bore.

The results show that the first response is indeed that of the flange bore and that it is easily distinguishable from all other responses. By simply measuring the angle and depth of this response, the required focusing distance and steering angles can be found.

From Figure 10, it can be identified that lobes near the probe are very prominent. It
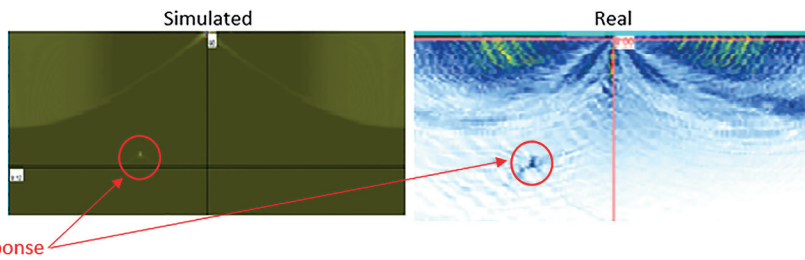
Figure 10. CIVA and real-world output

is reasonable to consider the possibility that these will potentially hide the bore response if it falls into an area affected by them. If this were to happen, no angle or depth measurements could be established. If this method is to be employed, its limitations of use must be determined.

3.4 Parametric study

To confirm the viability of the WSM, its capability across the full spectrum of possible flange geometries must be assessed. In order to achieve this, simulations are performed on five flange angles (10°, 20°, 30°, 40° and 50°). For each angle, five wall thicknesses, ranging from 5 mm to 25 mm in increments of 5 mm, are used.

By utilising these dimensions, it is ensured that the greatest and smallest angles permissible by the ASME B16.5 standard are included. This standard covers pressure-temperature ratings, materials, tolerances, marking, testing, methods of designating openings and, most importantly, dimensions for all pipe flanges and flanged fittings[9].

For each angle and thickness, a simulation is produced of the wide sweep to find the focal depth and steer parameters. Once obtained, these parameters are used firstly to simulate a sectorial scan with the centre at a normal to the bore and secondly to repeat the same S-scan but focused at the recorded bore depth.

3.5 Results of parametric study

Figure 11 shows a selection of the results taken from the simulation of a 5 mm wall thickness with a skirt angle of 10°. With the lowest angle and thinnest wall, it is the geometry that produces a bore response closest to the lobes. Despite this, there is still a significant distance between the lobes and the wide sweep calibration point. Due to this, and the fact that the measurements taken from this point allowed for correct steering angles and depths, it can be concluded that the WSM is applicable to all flange geometries.
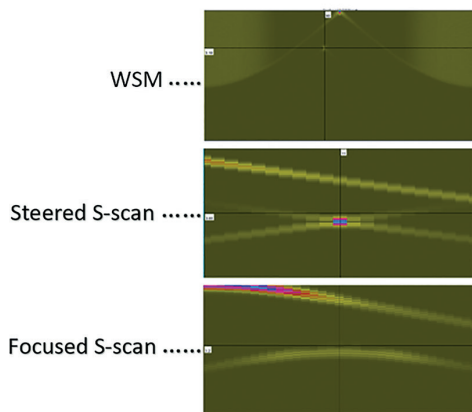

Figure 11. Parametric results

4. PAUT imaging methods

For the vast majority of applications, phased array technology is separated into two main inspection and imaging types: linear and sectorial. More modern techniques such as full matrix capture (FMC) combined with the total focusing method (TFM) are available. However, due to the extra data collection and computational needs, these techniques are currently slower to perform and often require bulkier and less portable equipment. It would be advantageous for the imaging technique used for flange bore inspection to be able to be performed on as many in-service and portable phased array units as possible. This would reduce the cost of implementation and ensure that testing can be achieved on less accessible pipelines, for example in an offshore environment.

4.1 Linear scanning

Linear scans are constructed by multiplexing a predetermined aperture along an array of elements[10]. Figure 12 shows how each scan is conducted at a fixed angle and focused to a given depth.
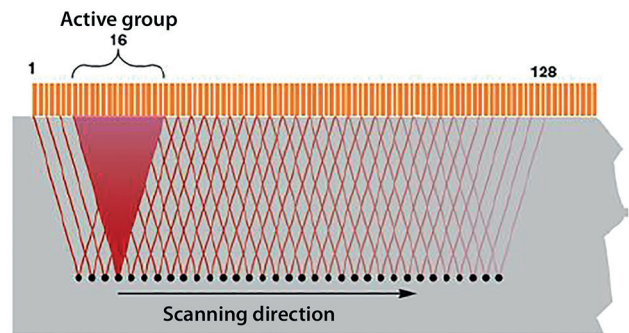

Figure 12. Linear scan multiplexing across 128 elements[10]

Most arrays used for inspection currently have between eight and 64 elements (although probes are available with up to 256). Linear scanning allows for a large area to be inspected while maintaining a tight focal spot. Typically, a flat and linear array is used to simply produce B-scan images. However, curved or even flexible probes are available[11].

Benefits of linear scans are their simplicity and ease of use while producing a scan image that is visually representative of the test-piece. Compared to conventional ultrasonic testing (UT), a linear scan can also greatly reduce inspection times. For example, a PAUT system operating in linear mode can use three channels to inspect a weld at each of the common conventional angles (45°, 60° and 70°) in a single pass rather than three.

4.2 Sectorial scans

Sectorial scans use a fixed aperture of elements throughout testing. Unlike a linear scan, sound is steered (or swept) through a range of angles, typically with 1° increments. The versatility and flexibility of sectorial phased array scans has led to them being the most commonly used method, not just within the NDT industry but also in the medical field[1]. Figure 13 shows a typical S-scan as produced by a sectorial sweep with a backwall and four side-drilled hole (SDH) manufactured defects.
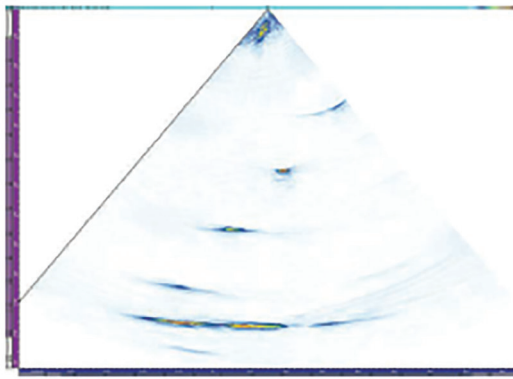
Figure 13. S-scan produced by a sectorial sweep[5]

The start and finish angles are dependent on the design of the probe, the wedge and the required coverage. S-scans are unique to phased array systems and offer excellent imaging and data interpretation with improved resolving power over conventional scanning[12].

4.3 Compound scanning

Consisting of multiple sectorial scans overlapped, summed and averaged, the compound scan technique combines many benefits of both linear and sectorial scanning while only marginally increasing the computational requirements of a system. Although used for many years in the medical field, the compound scan is a relatively new but growing inspection strategy within NDT. Currently, it is used almost exclusively for weld inspection in conjunction with an angled wedge. The wedge means that the lower portion of the active aperture generates a beam of a lower angle and the higher active aperture generates a beam of a higher angle. As can be seen in Figure 14, the compound S-scan generates a larger coverage area with this set-up, negating the need for two standard sectorial scans[3].

Figure 14. Compound and S-scan

Due to its make-up of multiple sectorial scans, it is theorised that this technique offers another benefit when testing on non-parallel surfaces. Although it is possible to focus a single sectorial scan at multiple depths through its range of angles, the origin of these focal spots will always be the centre of the aperture. When compounded, the same spots can be focused upon multiple times and from a varied range of angles, thus reducing the impact of defect orientation on signal response.

4.3.1 Compound scan generation

Although a varied focal distance is required, it is imperative that the centre of each individual S-scan within that of the compound is generated with a wavefront that is parallel to the surface being inspected. As can be seen in Figure 15, this will mean that the direction of propagation will be 90° to that of the flange bore.
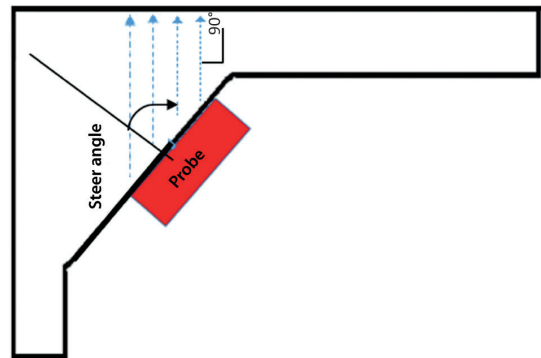

Figure 15. Required steering angle

Due to the varied nature of angles within a flange, it is useful to find a section that will remain uniform to provide a basis for the relevant formulae. One logical datum to take angular measurements is the bolt face. By subtracting the angle between the bolt face and the flange skirt (α) from 180°, the value for the angle at which steering must be performed (β) can be obtained. This is illustrated in Figure 16.
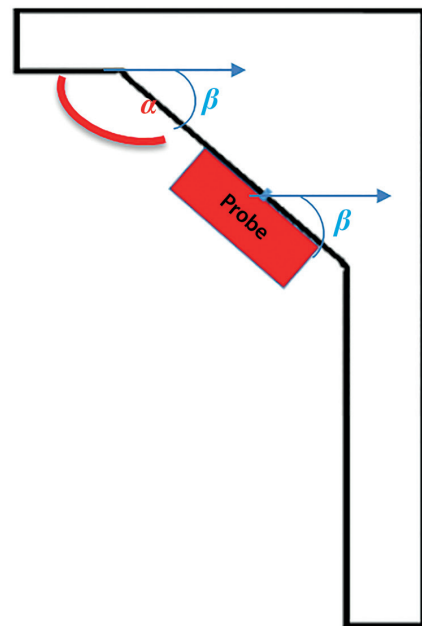

Figure 16. Delay angle

To calculate the delay laws, first the delay distance must be calculated. This is the amount by which the beam leaving the first element must travel before the second is fired in order to achieve the desired angle. By dividing this value by the velocity of sound, the required delay time is determined. The combined calculation is shown in Equation (1):

$$\text{Delay} = \frac{Ep.\sin(\beta)}{\text{Velocity}} \dots\dots\dots\dots\dots\dots\dots\dots (1)$$

The process is further complicated due to the requirement of focusing to produce high-quality imaging. Rather than a single wavefront, a focused beam is formed from multiple wavelets that converge at a designated spot.

By utilising the WSM, the angle and linear distance between the bore and the centre of the aperture are measured. Figure 17 and Equation (2) illustrate how it is possible to extrapolate the distance between the bore and any single element centre from these measurements as well as element pitch:

$$x = N.Ep.(\cos\beta) \quad\text{.....................................} (2)$$

where N is the number of elements from the centre, β is the bore-to-interface distance, β is the bore-to-interface angle and Ep is the element pitch.
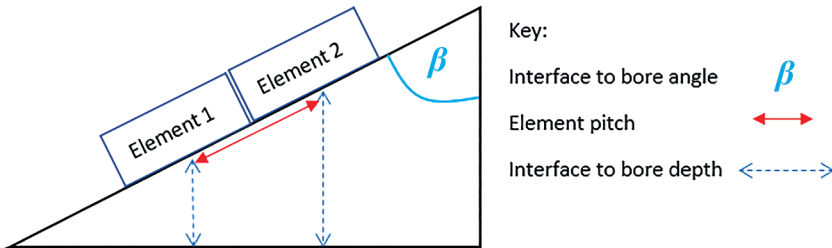

Figure 17. Multi-depth determination

When conducting compound scanning, it is possible to control the number of elements used in each individual sectorial scan. A higher element count will increase the maximum distance at which focusing can occur. This distance can be calculated with Equation (3):

$$Nf = \frac{k.F.(N.Ep)^2}{4.V} \quad\text{.....................................} (3)$$

where k is the width/length factor, N is the number of elements, Ep is the element pitch, F is the frequency and V is the velocity.

This formula is only viable when the width of the aperture is greater than that of the wavelength of the sound within the medium. As the secondary aperture of a LM 5 MHz probe is 10 mm and the compression wavelength in steel is approximately 1.2 mm, this will always be the case.

It would not be unreasonable at this point to assume that as high an element count as possible should be used in order to achieve the highest focal distance. In practice, however, higher numbers of elements result in fewer individual scans (Equation (4)), which in turn results in fewer angles for insonification, individual focal points and scan averaging. Consequently, there is a trade-off between the required focal ability and the number of individual scans.

As the wide sweep method determines the required focal distance, this can allow for the correct individual scan aperture to be selected:

$$N = (e-a)+1 \quad\text{.....................................} (4)$$

where N is the number of scans within the compound, e is the total number of elements within the probe and a is the number of elements in the individual scans.

5. Experimental evaluation

5.1 Set-up

In order to compare the effectiveness of compound scanning to contemporary linear and sectorial methods, an investigation is performed with the use of a Zetec Dynaray phased array unit and an LM 5 MHz 64-element probe. Although only one probe has been used in this experiment, in practice the probe selection is determined by the available length of the test surface and the

available space behind any protruding bolts. Due to the circular nature of the component and use of a flat probe, care was taken to minimise issues related to probe intimacy in the passive axis.

Two test samples have been inspected. The first was purpose-built duplex stainless steel flange with two manufactured defects. These defects were created by drilling 3 mm-diameter holes to a depth of 3 mm. As a new component this flange is in pristine condition (with exception of the holes).

In contrast, the second sample was a flange that was taken out of service due to a corroded face. Once removed from service the extent of corrosion within the bore was also seen to be excessive. The entirety of the internal surface is rough with light pitting. The external surface also has a paint layer that may cause complications. In previous testing, one particular pit of approximately 3 mm depth proved to be difficult to detect and has therefore been selected as the defect that will be scanned in this sample. The two samples along with the defects are shown in Figure 18.

The WSM technique is employed to determine the bore angle and depths before conducting sectorial, linear and compound scanning of each defect location. The aperture for both the wide sweep and the sectorial test will be the full array of 64 elements with an active aperture of eight elements used during linear and compound testing. No filtering or image smoothing is applied at any stage.

Figure 18. Test samples

5.2 Results

5.2.1 Sector scan

Figure 19 shows that an unfocused sector scan is unable to display the bore, let alone a defect, and therefore its suitability for testing non-parallel surfaces can instantly be disregarded.

Once focused, sector scanning is able to image some of the internal surface. One of the duplex defects (defect 2) and the pit within the carbon steel sample are also visible. However, these images are misrepresentative as the aspect ratio makes the area covered by the scan appear to be the same as that of the linear and compound scans shown in the next sections. In fact, for the same
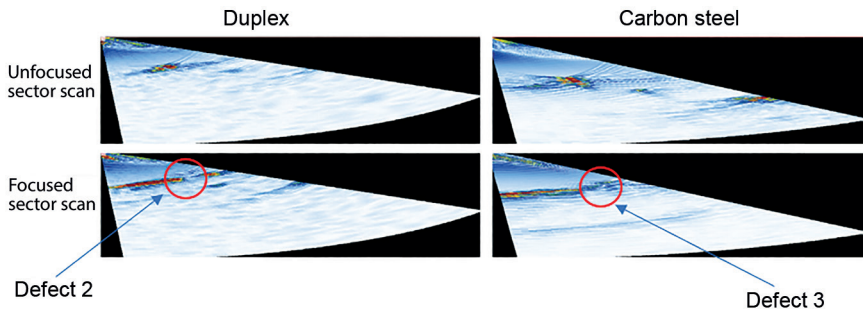
Figure 19. S-scan results

reason that the wide-angle sweep works to determine geometries, a sectorial scan will only be able to cover a very small area of a bore. Only the sweep angle at or close to perpendicular to the bore will return a signal. Even where the angle permits coverage of the defect, such as the case with defect 2, a poor response is received with the top of defect being unclear. In principle, although defect detection is possible with this imaging method, it would require many passes to cover the entire bore area and would not allow for accurate wall loss measurement.

5.2.2 Linear scan

In Figure 20, the results from the duplex sample appear to show that the linear scan is capable of detecting and imaging defects. Due to the straight edge of the drilled holes and their orientation, a strong corner response is returned. The defect closest to the pipe side is almost covered by the interface response. However, if filtering were to be used, it is likely that the impact of this response could be reduced, allowing for easier detection of defects in this region.

Looking at defect 3 within the carbon steel sample, the limit of this technique is made apparent. As only one angle is used if it does not line up with the defect, a very weak signal or no signal is returned. The shape of this defect is almost perfect to deflect sound away from the point of origin and this is why it was included in this study. As a major loss of backwall is observed, it would be possible to identify the presence of a discontinuity although no sizing would be achievable. An operator may alternatively mistake a loss of response to be due to coupling inconsistency and not make a defect call.

5.2.3 Compound scan

Unlike either of the cases involving linear or sectorial scanning imaging methods, all three defects are identifiable in this case. Due to multiple points of origin, each defect is insonified from an angle that allows for a signal to be returned to the probe. The improved visualisation means not only that it is easier to detect a defect, but also that its extent into the material can be measured.

As predicted in[2], the compound image has reduced noise. This allows for the identification of a defect closer to the surface than the linear scan without the need for filtering. Due to the rougher surface of the real-world flange, the interface suffers from a greater level of noise. Even so, Figure 21 shows

that, unlike in Figure 20, the defect located in the region near to the bore (defect 1) is readily distinguishable from the interface signal.

6. Conclusions and future work

From the work presented it is possible to draw the following conclusions:

- Simulations have shown that the WSM is capable of determining the angle and depth of a far surface without any previous knowledge of the geometry.
- The simulation results have been validated utilising results from physical testing.
- Sectorial and linear scanning methods have displayed inherent weaknesses when testing different defect types and non-parallel surfaces.
- The compound scan overcomes these weaknesses, allowing for detection, with the possibility of measuring a full range of defect types and orientation.
- Utilising the compound scan imaging technique in conjunction with the WSM, complete imaging of the bore and internal defects is achievable on flanges with unknown geometries.

Although within this paper it has been suggested that the compound scan allows for the measurement of defect depth, further study is required in order to assess the accuracy of any such measurement. If the proposed WSM and compound scanning techniques are to be deployed, then calibration standards must be set. This will require further study to establish reference standards and allow for the correct gain, filtering and aperture settings for various flange materials and geometries.
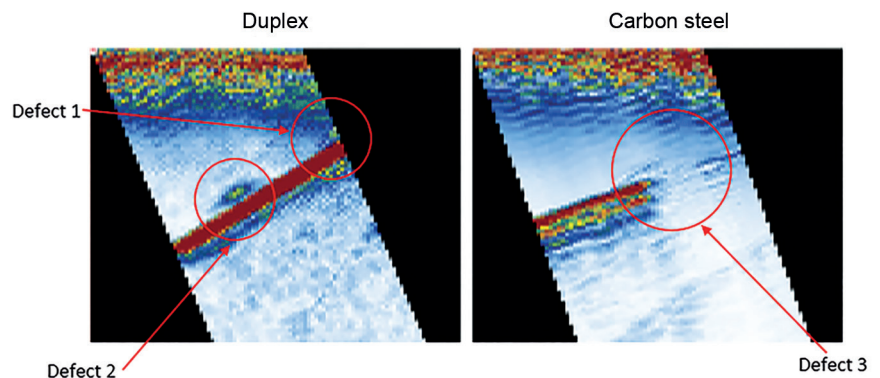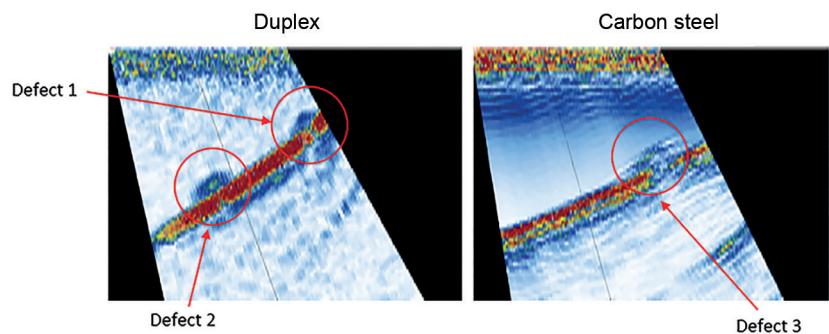

Figure 20. Linear results

Figure 21. Compound results

Once these standards are set, further investigation can then be made to quantify the detection and sizing capabilities of a compound scan that has been created using parameters found utilising the WSM.

Acknowledgements

References

1. S-C Wooh and Y Shi, 'Optimisation of ultrasonic phased arrays', Review of Progress in Quantitative Nondestructive Evaluation, Vol 17, pp 883-890, 1998.

2. D P Shattuck and O T von Ramm, 'Compound scanning with a phased array', Ultrasonic Imaging, Vol 4, No 2, pp 93-107, 1982.

3. Olympus, 'Improved scan plan strategy with compound S-scan for weld inspection', Olympus Industrial Resources, 2017. Accessed: 15 October 2017. Available at: https://www.olympus-ims.com/en/improved-scan-plan-strategy-with-compound-s-scan-for-weld-inspection

4. P R Dheeraj, 'Effect of focal law parameters on probability of detection in phased array ultrasonic testing using a simulation and case study approach', Materials Evaluation, Vol 74, No 11, pp 1574-1591, 2016.

5. S Kenny, 'The inspection of crevice corrosion in flange joints using manual phased array', Oceaneering Inspection, Swansea, Wales, 2012.

6. D Everheart and N Langley, 'Pipeline bursts: their causations and the deaths, bodily injuries and econominc and ecological damages they inflicted', US Department of Transportation, 2016.

7. J L Tischuk, 'Economics of risk-based inspection systems in offshore and gas production', Proceedings of COTEQ 2002, Salvador, Brazil, 2002.

8. Taylor Forge, Modern Flange Design: Bulletin 502, 1938.

9. ASME, 'Pipe flanges and flanged fittings: NPS 1/2 through NPS 24', 2017.

10. J M Davis and M Moles, 'Resolving capabilities of phased array sectorial scans (S-scans) on diffracted tip signals', Insight: Non-Detructive Testing and Condition Monitoring, Vol 48, No 4, pp 233-239, 2006.

11. M Zhafri, 'The detection of microbial attack corrosion using curved phased array technology', 2014.

12. R/D Tech, Introduction to Phased Array Ultrasonic Technology: R/D Tech Guideline, 2007.